

# Wet granulation multiscale modelling accelerated via CG-DEM

Roxana Saghafian Larijani<sup>1,\*</sup>, Stefan Luding<sup>2,\*\*</sup>, and Vanessa Magnanimo<sup>1,\*\*\*</sup>

<sup>1</sup>Department of Civil Engineering and Management, Faculty of Engineering Technology, University of Twente, Enschede, Netherlands

<sup>2</sup>Department of Thermal and Fluid Engineering, Faculty of Engineering Technology, University of Twente, Enschede, Netherlands

**Abstract.** Wet agglomeration is a complex particulate process driven by multiple microscale mechanisms. Discrete Element Modeling (DEM) enables a deeper understanding of these mechanisms and supports process optimization. However, DEM simulations become computationally expensive at larger scales. Moreover, identifying granules within dense systems remains challenging.

This study introduces a framework for granule identification using Graph Network Analysis (GNA). To enhance computational efficiency, a Coarse-Grained (CG) DEM approach is implemented. The accuracy of the CG up-scaling by factors 2 and 3 is first validated against the original system (CG1) to ensure it effectively reproduces the granulation characteristics. Leveraging the speed of CG-DEM, this sets the basis for studying the effects of other material and process parameters (e.g. surface tension and rotation speed) on key granulation metrics like mean granule volume, size distribution or granulation yield.

## 1 Introduction

Wet granulation is widely used in industries such as pharmaceutical, food, and chemical processes to enhance powder flowability, minimize segregation, and improve downstream product properties. The granule size distribution (GSD) is a key characteristic influencing product quality. However, optimizing granulation through experiments alone is costly and time-consuming, making computational approaches essential [1].

Discrete Element Modelling (DEM) has become a popular tool for studying powder systems, such as granulation. However, directly extracting GSD remains a challenge, as it is important to set criteria to differentiate between the particles in collision and the ones firmly agglomerated. Population Balance Modelling (PBM) is often coupled with DEM to estimate the GSD. Alternative methods include virtual sieving [2] and density-based clustering techniques like DBSCAN [3]. On the other hand, network analysis has also been integrated with DEM to investigate force chains and particle motion [4, 5], while its application to granule identification remains underexplored.

A major drawback of DEM is its high computational cost, especially for large-scale problems. Coarse-Grained DEM (CG-DEM) offers a potential solution [6]. Previous studies have extended DEM-PBM frameworks to CG-DEM-PBM [7], but the effects of CG-DEM on granulation characteristics remain poorly understood.

This study applies graph network analysis (GNA) to identify clusters in a baffled drum granulator, as described

in Sec. 2. With appropriate scaling rules used for the different upscaled systems, number, volume and size distribution of the granules, as well as the granulation yield are compared to the original simulations in Sec. 3.1. Finally, the influence of cohesion and rotation speed is analyzed using the CG-DEM-GNA framework in Sec. 3.2.

## 2 Modelling

The Discrete Element Method (DEM), see [8, 9] and references therein, is widely used for simulating granular systems by tracking individual particle trajectories based on Newton's second law. In this study, DEM simulations are conducted using the open-source software YADE [10].

The governing equations of motion for the particles are:  $m_i \frac{dv_i}{dt} = \sum_j f_{ij} + m_i g$ , and  $I_i \frac{d\omega_i}{dt} = T_i$ , where  $m_i$  and  $I_i$  represent the mass and moment of inertia of particle  $i$ , respectively, while  $v_i$  and  $\omega_i$  denote its translational and angular velocities. The forces acting on the particle include contact force  $f_{ij}$  between particles  $i$  and  $j$  and gravitational force  $m_i g$ , with  $T_i$  representing the total torque on  $i$ .

A linear viscoelastic contact model is employed, incorporating the capillary liquid bridge model by [11] for normal forces and a viscoelastic slider for tangential interactions. Further details on the contact model can be found in our previous work [9]. Parameters are summarised in table 1.

The original particle simulations involve 120000 particles with a homogeneous size distribution within the range  $d_o - 0.2d_o < d < d_o + 0.2d_o$ , with the original particle mean diameter  $d_o$ . In CG simulations, all particle sizes are scaled by a factor  $\alpha$  and particle numbers by a factor  $1/\alpha^3$ .

A central cylindrical spray zone ( $V_s$ ) of radius  $r_s = 0.063$  m is defined in the simulations where liquid is pe-

\*e-mail: r.saghafianlarijani@utwente.nl

\*\*e-mail: s.luding@utwente.nl

\*\*\*e-mail: v.magnanimo@utwente.nl

Table 1: Default parameters used in the DEM simulations

|   |                           |
|---|---------------------------|
| Particle density ( $\rho$ )               | 2500 [kg/m <sup>3</sup> ] |
| Original particle mean diameter ( $d_o$ ) | 0.0015 [m]                |
| Normal contact stiffness ( $k_n$ )        | 150 [N/m]                 |
| Tangential contact stiffness ( $k_t$ )    | 120 [N/m]                 |
| Damping coefficient ( $c_n, c_t$ )        | 0.0011 [Ns/m]             |
| Liquid surface tension ( $\gamma$ )       | 0.1095 [N/m]              |
| Liquid viscosity ( $\eta$ )               | 0.0015 [Pa s]             |
| Contact angle ( $\theta$ )                | 0 [°]                     |
| Coefficient of friction ( $\mu_p$ )       | 0.5 [-]                   |
| Time step ( $\Delta t$ )                  | $3 \times 10^{-6}$ [s]    |
| Drum angular velocity ( $\omega$ )        | 2 [rad/s]                 |

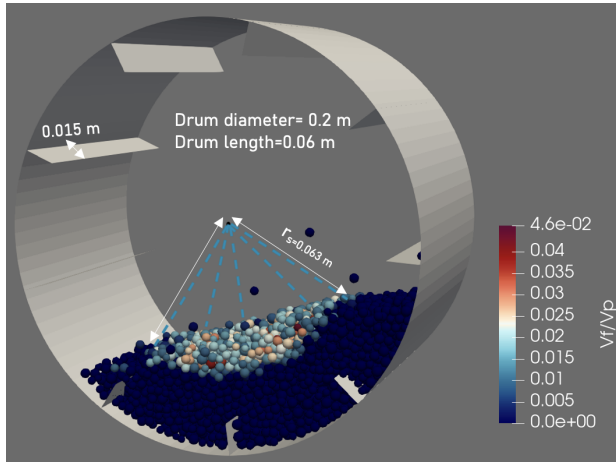


Figure 1: Snapshot of the drum granulator with the defined spray zone  $r < r_s$ . The colour bar indicates the ratio of liquid film volume to the particle volume.

riodically introduced. Liquid spraying occurs every 0.2 seconds, with each spray adding  $0.01V_p$  to the liquid film  $V_f$  at each particle within  $V_s$ . The spray zone dimension remains unchanged in the CG simulations. Figure 1 illustrates the geometry of the granulator and the dimensions of the spray zone. To account for liquid migration among wet particles, the model proposed by Mani et al. [12] is used.

## 2.1 CG-DEM

To enhance the computational efficiency of simulations, coarse-grained (CG) particles are used to represent groups of original particles, with scaling rules applied to preserve the systems behaviour. An extensive review of CG-DEM studies on wet granular systems can be found in [9]. Table 2 summarizes the scaling rules based on Weber-number-based scaling [13, 14], with  $We$  as the ratio of the kinetic energy density to the capillary stress as  $We = \frac{\rho_p R_p v^2}{\gamma \cos \theta} = \frac{\rho_p R_p (\Omega D)^2 / 4}{\gamma \cos \theta}$ , where  $R_p$  is particle radius, and  $v = \Omega D / 2$  is the velocity of the flowing particles, estimated as the angular velocity of the drum,  $\Omega$ , times the drum radius,  $D / 2$ .

Table 2: The Weber-based coarse-graining rules [9]

| Parameters      | $\gamma$ | $\eta$   | $k$      | $c$        | F          |
|-----------------|----------|----------|----------|------------|------------|
| Scaling factors | $\alpha$ | $\alpha$ | $\alpha$ | $\alpha^2$ | $\alpha^2$ |

## 2.2 Graph analysis via Breadth first Search algorithm (BFS)

A post-processing tool for granule identification is developed using the NetworkX Python library [15]. After the contact network is identified, groups of particles are considered to be in a granule if:

1) The cohesion among the particles is strong enough, i.e.  $F_{coh} \geq F_{agg}$ , the normal cohesive force between particles  $i$  and  $j$  is larger-equal to a threshold  $F_{agg}$ . Based on the maximum capillary force in the system,  $F_{coh}^{max} = 2\pi\gamma R_p$ , the threshold is defined as  $F_{agg} = C_{agg} F_{coh}^{max}$ , where  $C_{agg}$  is the threshold coefficient.

2) The angle between the velocity vectors ( $v$ ) or between the angular velocity vectors ( $\omega$ ) of the particles  $i$  and  $j$  is smaller than a threshold angle,  $A_{agg}$ . This ensures collective translational or rotational motion of the granule.

The Breadth-First-Search (BFS) algorithm in NetworkX is then used to identify connected particles forming granules within the system, based on the filtered contacts. Figure 2 shows the schematic of the granule detection.

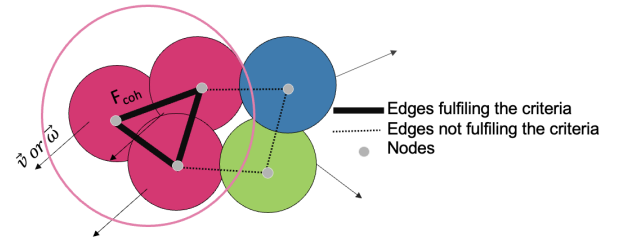


Figure 2: Schematic of cluster detection using graph analysis. The red circle demonstrates a formed granule, arrows indicate particle velocity.

The analysis in the next sections uses  $C_{agg} = 0.6$  and  $A_{agg} = 20^\circ$ . The sensitivity of the granule size distribution to the abovementioned thresholds is investigated in [16]. Calibration via experiments is subject of ongoing research.

## 3 Results and discussion

### 3.1 Effect of CG on granulation

In this section, the effect of coarse-graining on the mean granule size, number of granules, particle size distribution of granules, and granulation yield is investigated. The thresholds for the CG simulations are scaled as:  $F_{agg,CG} = \alpha^2 F_{agg,o}$ , as  $R_p$  and  $\gamma$  scale  $\alpha$  times in the CG system, and  $A_{agg,CG} = A_{agg,o}$ .

Figure 3 shows the evolution of the normalized mean granule volume for CG1, CG2, and CG3. To be able to

compare different cases, the mean granule size is normalized with the mean particle volume. The results show that, with addition of water, the volume of the granules first increases and then stabilizes, due to water redistribution. The growth behavior is similar between different CGs and the final normalized mean volume of the granules agrees well, being only slightly smaller for larger CG.

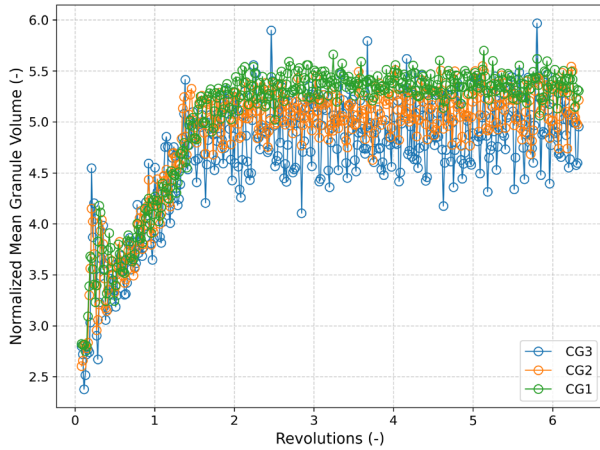


Figure 3: Effect of CG on the normalized average volume of the granules

The evolution of the number of granules in systems CG1, CG2, and CG3 is presented in Figure 4, normalized by the initial number of particles. The results show a convincing agreement between the normalized number of granules in original and CG systems with slightly more granules for larger CG.

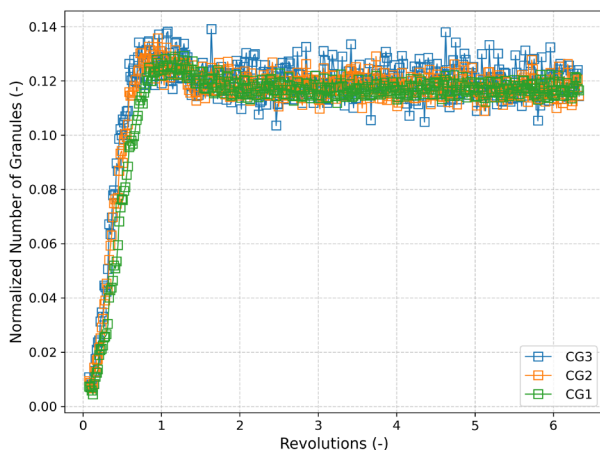


Figure 4: Effect of CG on the number of granules

The probability distribution of the number of particles in each granule averaged over revolutions  $\in [2 : 6]$  are compared in Figure 5. It can be observed that for the granules with less than approximately 20 particles, the probability distributions collapse. Over two orders of magnitude, however, as the number of particles per granule increases, the statistics of CG2 and CG3 deteriorate and data fluctuate more, and consequently deviate from the original

case. This suggests that when using CG modelling, data might lose information details.

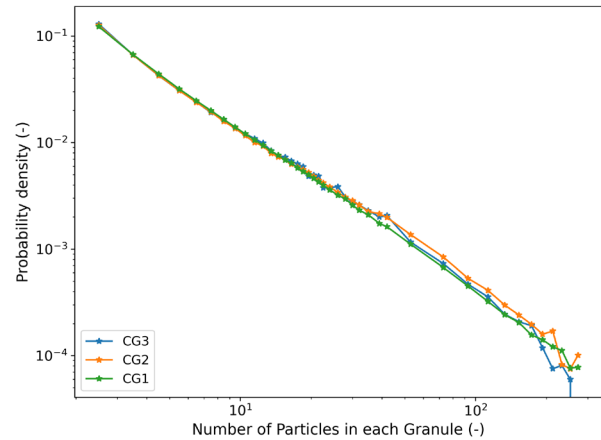


Figure 5: Number of particles in each granule averaged over steady state revolutions  $t_R \in [3 : 6]$ .

The evolution of the fraction of granulated particles, i.e., process yield is presented in Figure 6. The growth rate is high at the beginning, dropping at one revolution and vanishing after two. Different CG cases are in good agreement, with higher fluctuations in CG2 and CG3. All CG systems reach a final granulation yield slightly above 55%.

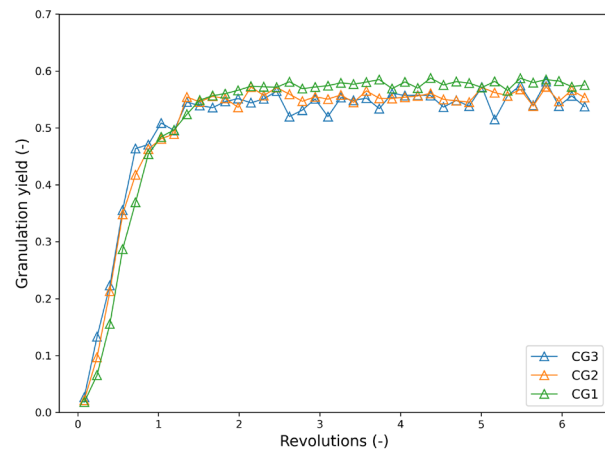


Figure 6: Evolution of the granulation yield

### 3.2 Effect of material and process parameters

Finally, the effect of rotation speed and liquid surface tension on the mean volume of the granules is presented in Figure 7 for CG2. With increasing surface tension, the mean granule volume increases at all rotation speeds as  $\langle V_g \rangle / V_p = \beta(\gamma - \gamma_1)$ , with slope  $\beta \approx 70$  and lower limit  $\gamma_1 \approx 0.027$ . At small surface tensions  $\gamma \leq \gamma_1$ , there are no considerable granules found. All data collapse reasonably well for different rotation speeds and a wide range of  $\gamma$ . Only at the highest  $\gamma = 0.4440$  N/m, the mean volume of

granules increases slightly with decreasing rotation speed.

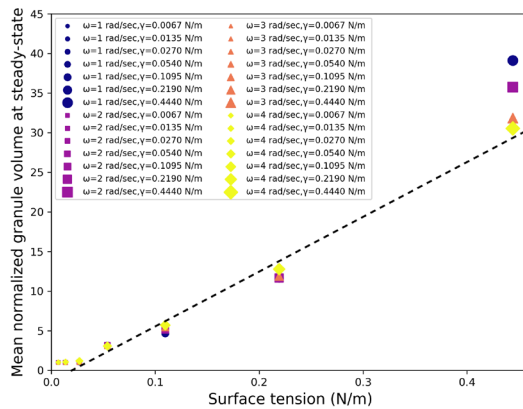


Figure 7: Effect of rotation speed,  $\omega$ , surface tension,  $\gamma$ , on the mean volume of granules in steady-state, from the CG2 system simulations with  $\gamma_2 = 2\gamma$ .

## 4 Conclusion

In this study, we employed CG-DEM to model a drum granulator and graph network analysis (GNA) to identify granules based on cohesive force and velocity criteria. By comparing key metrics, including mean granule volume, number of granules, granule size distribution, and process yield, we observed good agreement of upscaled CG simulations with the original case, while achieving approximately 12 $\times$  and 32 $\times$  speed-up for CG2 and CG3 simulations, respectively. Therefore, the proposed CG-DEM framework, integrated with graph network analysis, enables a trade-off between simulation efficiency and accuracy, making it a valuable tool for investigation of a complex process such as granulation. Studying alternative GNA-criteria and developing a model for predicting granulation characteristics, via integrating machine learning models in this framework, is subject of future studies.

## 5 Acknowledgements

This research is part of the project TUSAIL and has received funding from the European Horizon2020 program under grant agreement ID 955661.

## References

[1] M. Singh, S. Shirazian, V. Ranade, G.M. Walker, A. Kumar, Challenges and opportunities in modelling wet granulation in pharmaceutical industry—a critical review, *Powder Technology* **403**, 117380 (2022).

[2] X. Shi, C. Li, Q. Wang, G. Li, W. Zhang, Z. Xue, Numerical study of the dynamic behaviour of iron ore particles during wet granulation process using discrete element method, *Powder Technology* **401**, 117296 (2022).

[3] M. Dong, Z. Wang, B. Marks, Y. Chen, Y. Gan, Partially saturated granular flow in a rotating drum: The role of cohesion, *Physics of Fluids* **35**, 11 (2023).

[4] D.S. Bassett, E.T. Owens, M.A. Porter, M.L. Manning, K.E. Daniels, Extraction of force-chain network architecture in granular materials using community detection, *Soft Matter* **11**, 2731 (2015).

[5] R. Navakas, A. Džiugys, E. Misiulis, G. Skarbalius, Identification of collective particle motion in a rotating drum using a graph community detection algorithm, *Mathematical Methods in the Applied Sciences* **45**, 8864 (2022).

[6] M. Sakai, S. Koshizuka, Large-scale discrete element modeling in pneumatic conveying, *Chemical Engineering Science* **64**, 533 (2009).

[7] T. De, A. Das, M. Singh, J. Kumar, Enhancing efficiency in particle aggregation simulations: Coarse-grained particle modeling in the dem-pbm coupled framework, *Computer Methods in Applied Mechanics and Engineering* **417**, 116436 (2023).

[8] P. Cundall, O. Strack, Discussion: A discrete numerical model for granular assemblies, *Géotechnique* **30**, 331 (1980).

[9] R.S. Larijani, V. Magnanimo, S. Luding, A coarse-grained discrete element model (CG-DEM) based on parameter scaling for dense wet granular system, *Powder Technology* **453**, 120581 (2025).

[10] V. Smilauer, V. Angelidakis, E. Catalano, R. Caulk, B. Chareyre, W. Chevrement, S. Dorofeenko, J. Duriez, N. Dyck, J. Elias et al., Yade documentation, arXiv:2301.00611 (2023).

[11] C.D. Willett, M.J. Adams, S.A. Johnson, J.P. Seville, Capillary bridges between two spherical bodies, *Langmuir* **16**, 9396 (2000).

[12] R. Mani, D. Kadau, H.J. Herrmann, Liquid migration in sheared unsaturated granular media, *Granular Matter* **15**, 447 (2013).

[13] J. Tausendschön, J. Kolehmainen, S. Sundaresan, S. Radl, Coarse graining Euler-Lagrange simulations of cohesive particle fluidization, *Powder Technology* **364**, 167 (2020).

[14] E.L. Chan, K. Washino, Coarse grain model for DEM simulation of dense and dynamic particle flow with liquid bridge forces, *Chemical Engineering Research and Design* **132**, 1060 (2018).

[15] A. Hagberg, D. Conway, NetworkX: Network analysis with python, <https://networkx.github.io> (2020).

[16] R.S. Larijani, S. Luding, V. Magnanimo, CG-DEM modelling of drum granulation process: Effect of CG on granulation characteristics, To be submitted (2025).